Journal of Constructional Steel Research 65 (2009) 1836–1845

Contents lists available at ScienceDirect

Journal of Constructional Steel Research

journal homepage: www.elsevier.com/locate/jcsr

Strength deformation behaviour of circular concrete filled steel tubes subjected to pure bending

Manojkumar V. Chitawadagi *, Mattur C. Narasimhan [1]

Department of Civil Engineering, National Institute of Technology Karnataka, Surathkal, Mangalore-575025, India

ARTICLE INFO

Article history:
Received 10 June 2008
Accepted 12 April 2009

Keywords:
Concrete-filled steel tubes
Beams
Circular tubes
Flexural strength
Flexural stiffness

ABSTRACT

The strength deformation behaviour of circular steel tubes filled with different grades of concrete under flexure is presented. The effects of steel tube thickness, the cross sectional area of concrete, strength of in-filled concrete and the confinement of concrete on moment capacity and curvature of Concrete Filled steel Tubes (CFTs) are examined. Measured flexural strengths are compared with the values predicted by EC4-1994 and LRFD-AISC-1999 code provisions. A total of ninety nine specimens, all one metre long, were tested with concrete fills of 20, 30 and 40 N/mm^2 characteristic strength and with D/t ratio 22.3 to 50.8. Based on the experimental results, an interaction model to predict moment and curvature of the CFT sample is developed.

1. Introduction

Composite members consisting of circular or rectangular steel tubes filled with concrete are being extensively used in structures involving very large applied moments, particularly in zones of high seismic risk. Concrete Filled Tubes (CFTs) have been used as columns and beam–columns in braced and unbraced frame structures [1]. A steel hollow section in-filled with concrete has higher strength and larger stiffness than the conventional structural steel section and reinforced concrete [2]. While there is a large number of studies on the behaviour of CFT columns and beam–columns; there is relatively little research reported on the flexural behaviour of concrete-filled hollow structural steel beams [3]. The structural behavior of a CFT is governed by the member strength, reflecting the fact that the load resistance is dependent not only on the material properties but also on the geometric properties of the entire member [4].

Tests on CFTs by Bridge [4] showed that the concrete core only provides approximately 7.5% of the capacity in members under pure bending. Lu and Kennedy [5] performed tests on twelve beams of concrete-filled Steel Square and Rectangular Hollow Sections for examining the effects of different depth to width ratios and different values of shear span to depth. The tests showed that the ultimate flexural strengths of the composite beams are increased by about 10%–30% over that of bare steel sections, depending on the relative proportions of steel and concrete. Uy [6] reported five beam tests on concrete-filled steel SHS. The test specimens were selected for examining the effects of different width-to-wall thickness ratios (from 40 to 100) and different concrete cylinder strengths (38 and 50 MPa). The tests showed that CFT beam members had a significant yielding plateau, and exhibited adequate ductility. Elchalakani et al. [1] presented an experimental investigation of the flexural behaviour of circular concrete-filled steel tubes (D/t = 12–110) subjected to large deformation pure bending. It was found that in general, concrete filling of the steel tube enhances strength, ductility and energy absorption especially for thinner sections. Han [3] proposed a mechanics model that can predict the behaviour of concrete-filled hollow structural sections. A. Elremaily and A. Azizinamini [7] from their experimental studies concluded that AISC-LRFD [8] provisions for calculating the capacity of CFT beam–columns are very conservative.

It is obvious that the key issue in understanding the composite structural behaviour of CFT sections under flexure is the interaction between the concrete core and the steel tube. In this paper, results of an extensive experimental study on circular CFTs under flexure are reported and are discussed. CFTs with three different diameters each with three different wall thicknesses (Table 1) are selected (D/t = 22.3–50.8). Three different grades of concrete in-fills are considered. An effort is made to find the relative contributions of the steel tube and the confined concrete core to the moment capacity and curvature of CFTs under flexure. Based on experimental results a simple regression model and an interaction model are proposed to calculate the moment capacity and the corresponding curvature of CFTs under pure bending.

* Corresponding author. Tel.: +91 8242474051; fax: +91 8362374985; mobile: 919449837148.

E-mail addresses: manojkumar1966@gmail.com, mvc@bvb.edu, manojkumar1966@rediffmail.com (M.V. Chitawadagi), mattur_cn@yahoo.com (M.C. Narasimhan).

[1] Tel.: +91 8242474051; mobile: 919449163427.

0143-974X/$ – see front matter © 2009 Elsevier Ltd. All rights reserved.
doi:10.1016/j.jcsr.2009.04.006

Nomenclature

A_c	Cross-sectional area of the concrete core
A_s	Cross-sectional area of the steel
D	Outer diameter of the steel tube
d	Inner diameter of the steel tube
G	Cube strength of the in-fill concrete
f_{ck}	Characteristic compressive strength of concrete
f_{scy}	Nominal yielding strength
f_y	Yield stress of steel
M_{ue}	Maximum test moment
M	Moment
M_{pred}	Predicted Moment
t	Wall thickness of the steel tube
W_{scm}	Section modulus of the composite beams
Φ_{ue}	Curvature at ultimate point for test sample
Φ_{pred}	Predicted Curvature at ultimate point
ξ	Confinement factor

2. Experimental programme

2.1. Concrete

Design concrete Mixes with characteristic strengths of 20, 30 and 40 MPa using locally available Portland Pozzolana Cement (PPC), crushed granite jelly (12 mm down) and river sand are used in the present investigation. Mix designs of these three grades of concrete are made based on the guidelines of IS 10262-1978 [9]. The mix proportions adopted for the three grades of concrete and 28 days cube strength determined in the laboratory for these mixes is shown in Table 2. Since the steel tube openings are small in size, in order to ensure proper compaction, a higher degree of workability i.e. 80–100 mm slump is adopted for the concrete mixes. This is accomplished by using silica fume and a super plasticiser as admixtures. Standard 100 mm solid cubes are used to test the compressive strength of the concrete.

2.2. Steel tubes

Mild steel tubes, cold-formed with yield strength of 250 MPa and 1000 mm long are used in the present investigation. These tubes are seam welded and the edges of the tubes are finished. The outer surfaces of the steel tubes are painted to avoid corrosion. The insides of the tubes are wire brushed to remove any rust and loose debris present. The deposits of grease and oil, if any, are cleaned away. The allowable D/t ratio of the steel hollow sections is less than the limits specified in Eurocode 4 (EC4)-1994 [10] to avoid premature buckling failure of CFT specimens.

2.3. Preparation of CFT samples

Steel tubes are kept in an upright position in the stand specially prepared for the casting of the specimen. The bottom ends of the steel tubes are tightly covered with polythene sheet and concrete is poured from the top. Concrete is filled in the steel tubes in approximately four (250 mm) equal layers and each layer is compacted with 25 blows from a steel rod. The top of the concrete is trimmed off using a trowel and the steel tube is kept undisturbed until it is taken out from the stand after 24 h to keep water in for curing.

2.4. Test set up and procedure

The specimens are tested at an age of 28 days. Flexure test specimens are tested in a 200 kN capacity loading frame. In the test setup at each load point and at the supports of the specimen a set of rollers is placed to allow free rotation. Thus the beam specimens are tested under a simple support condition. The load is applied along two lines spaced at one third of the effective span from either support. The axis of the specimen is carefully aligned with the axis of the loading device. Linearly Varying Displacement Transducers (LVDT) are placed at mid-span and at the two loading points. The ends of test specimen in-filled with concrete are left uncapped to allow slippage between the concrete and the steel tube. This is considered to be the worst case, although it might be deemed as being too unfavourable. Prior to the actual tests, a load level of 1–3 kN is applied and released to see that the LVDT displays are stable. The load is increased gradually until the specimen fails and the maximum load applied to the specimen during the test is recorded and the corresponding ultimate moment capacity is calculated. LVDT readings are recorded at appropriate load increments and the lateral deflection of the middle segment of the test beam subjected to pure bending is calculated using LVDT data as detailed below.

δ_1 and δ_2 are the deflections under the point loads applied on the test beam.

δ_m is the deflection at the mid-span of the test beam.

Then net deflection (δ_n) of the pure bending segment of the test beam is given by

$$\delta n = \delta m - \left(\frac{\delta 1 + \delta 2}{2}\right).$$

Table 1
Details of test samples.

Outer diameter of the steel tube (mm)	Wall thickness (mm)	
$D_1 = 44.45$	$t_1 = 1.25$	For each diameter of the tube
$D_2 = 57.15$	$t_2 = 1.6$	
$D_3 = 63.50$	$t_3 = 2.0$	

3. Results and discussions

3.1. Prediction of the moment capacity and curvature values (Design of experiments approach)

In view of saving time and material cost in experimentation, a lesser number of experiments is desired. Therefore, it is aimed to introduce the Taguchi method [11] to find a proper combination of process conditions and to analyse the results with minimum experimentation. The present work is intended to study the effect of three parameters (tube diameter, wall thickness and concrete grade) at three levels on the moment carrying capacity and curvature of the CFT beams with the help of the Design Of Experiments (DOE) approach. An orthogonal array helps in determining how many trials are necessary and the factor levels for each parameter in each trial. An L9-orthogonal array is selected which reduces to nine experimental evaluations (Table 3) and a set of combination of levels is obtained from MINITAB-14. Therefore nine experiments are initially conducted according to a combination level for CFT beams with an effective span of 850 mm and the corresponding experimental results are shown in Table 3.

After performing experiments as per L9-orthogonal array, the main effect plots for moment and curvature are plotted. A main effect is the direct effect of parameters on response or dependent variable. Figs. 1 and 2 show the main effect plots of parameters with respect to ultimate moment and associated curvature for circular CFT beams. They are plotted by considering the means of responses at each level of the parameters, as shown in Table 4. Analysis of the experimental results is also carried out, using the ANalysis Of VAriance (ANOVA) technique [11]. From Figs. 1 and 2, it can be noted that increase in any of diameter, or wall thickness will increase the moment carrying capacity. The diameter of the

Table 2
Concrete mix proportions.

Sl. no	Mix designation	Binder (B) (kg/m^3)		Proportions B:FA:CA	W/B ratio	Super plasticiser (%) (by wt of binder)	28 days compressive strength (G) (N/mm^2)	Slump (mm)
		Cement	Silica fume					
1	M_{20}	370	–	1:1.98:2.51	0.55	1.0	27.8	100
2	M_{30}	390	20	1:1.80:2.28	0.45	2.0	42.0	90
3	M_{40}	410	20	1:1.76:2.16	0.40	2.2	51.0	80

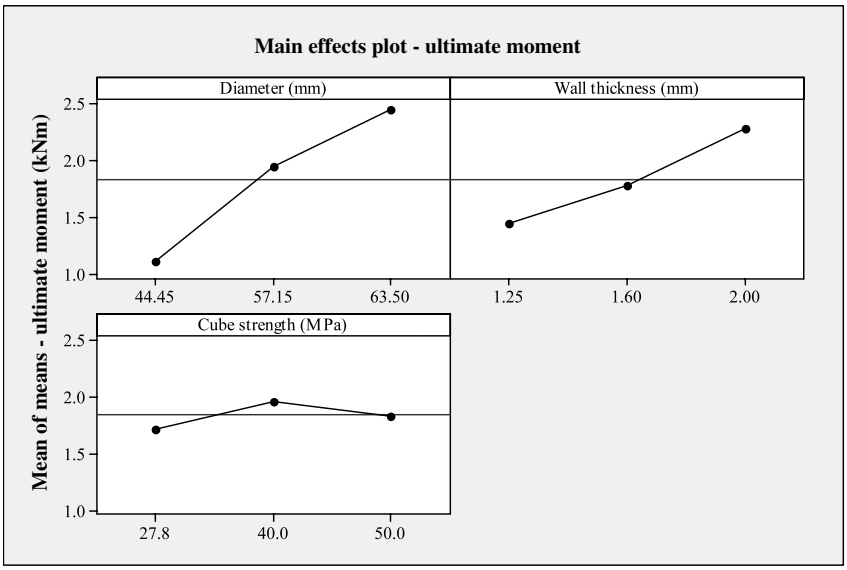

Fig. 1. Main effects plot—ultimate moment.

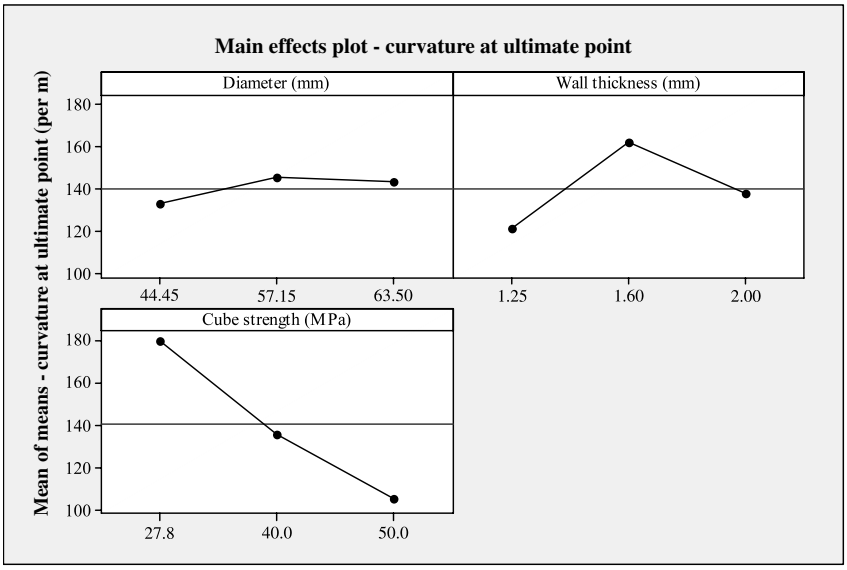

Fig. 2. Main effects plot—curvature at ultimate point.

steel tube has the most significant effect on ultimate moment capacity, while the strength of the concrete proves most significant parameter affecting the curvature of the CFT. To assess the rank of each of the parameters, the deltas of the means of each level of all the factors are calculated and are shown in Table 4. The Delta means the value of the maximum mean minus the minimum one. The most influencing factor is that which ranks first in the group. This is confirmed using results of the ANOVA technique presented in Table 5. A greater F value confirms that the diameter is the most influential factor among other factors on moment capacity of CFTs.

After conducting the initial nine experiments regression models are developed (Table 6). These models are used to predict the ultimate moment carrying capacity and associated curvature of the all other CFT samples in the experimental programme. To verify the accuracy of such predictions of the ultimate moment carrying capacity and associated curvature, actual bending tests are now conducted and a comparison of actual experimental values is made with the predicted values (Table 7). It is found that the regression models predict the moment carrying capacity of the circular CFTs, very well and reasonably well for the curvature (Table 7). Hollow samples are also tested to determine the advantage of concrete filling on moment capacity and associated curvature.

Table 3
L9 — Orthogonal array adopted and experimental results.

Sample designation	Ultimate moment M_{ue} (kN m)	Curvature at ultimate moment Φ_{ue} (m^{-1})
$D_1t_1M_{20}$	0.74	157.44
$D_1t_2M_{30}$	1.16	141.07
$D_1t_3M_{40}$	1.46	100.14
$D_2t_1M_{30}$	1.57	126.53
$D_2t_2M_{40}$	2.03	135.26
$D_2t_3M_{20}$	2.25	173.68
$D_3t_1M_{40}$	2.03	80.46
$D_3t_2M_{20}$	2.18	208.51
$D_3t_3M_{30}$	3.16	140.10

Note: Values are average of three samples.

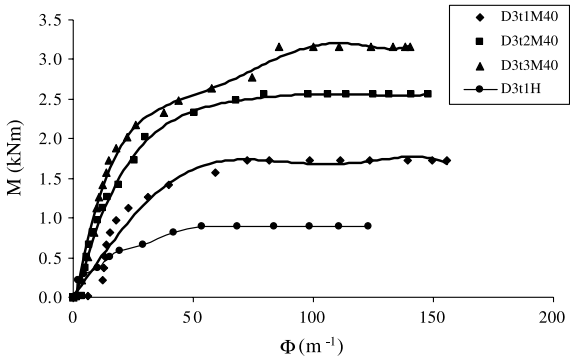

Fig. 3. Typical moment curvature relationship for CFT samples.

3.2. Effect of different parameters on ultimate moment capacity

CFT beams under flexure have behaved in a relatively ductile manner due to concrete in-fill and testing in general, proceeding in a smooth and controlled way. Typical moment–curvature curves obtained during the experiments (Fig. 3) clearly show the elastic and post yield behaviour of hollow and CFT elements. CFT beam samples exhibited a significant yield plateau.

From the experimental results it is observed that there is a significant increase in moment carrying capacity due to concrete filling of hollow sections, but there is no appreciable increase in moment resistance due to an increase in the strength of in-filled concrete from M_{20} to M_{40}. In-filled concrete helps in enhancing the section modulus of the composite section. The void filled concrete participates in increasing the moment of resistance of the section by taking compressive stress induced due to flexure in the compression zone. A parameter called **Strength Increasing Factor (SIF)** is now introduced to account the enhanced moment capacity due to composite action in CFT beams.

$$SIF = (M_{\mathrm{CFT}} - M_{\mathrm{Hollow}})/M_c \quad (1)$$

where M_c is defined as theoretical moment capacity of concrete core alone

$M_c = \frac{\pi d^3}{32}.f_{cr}$ for Circular CFTs; d = inner diameter of the steel tube; f_{cr} = allowable bending stress in concrete in tension [12] = $0.7\sqrt{f_{ck}}$; f_{ck} = characteristic strength of concrete N/mm^2; M_{Hollow} = experimental moment capacity of Hollow steel tube samples; M_{CFT} = experimental moment capacity of CFT samples.

From Fig. 4 it is observed that there is a nonlinear variation between D/t and the contribution of concrete for composite action in a CFT. But SIF is more for a given D/t ratio for CFT samples with M_{30} concrete as compared to those filled with M_{20} and M_{40} grades. Hence the use of high strength concrete as an in-fill in a CFT seems to be of not much advantage, under flexure. This is in agreement with the test results obtained by W.M. Gho and Dalin Liu [2] and Lu and Kennedy [5].

The ratio ($M_{\mathrm{CFT}}/M_{\mathrm{Hollow}}$) indicates the advantage of concrete filling in a hollow steel section (Table 8). It is found that the

Table 6
Regression analysis models for ultimate moment and curvature in terms of diameter, wall thickness and cube strength for nine experiments.

Regression model		
	Ultimate moment (kN m)	$M_{pred} = -4.03 + 0.0695D + 1.13t + 0.00578G$ $R^2 = 95.9\%$ $R^2_{adj} = 93.4\%$
	Curvature (m^{-1})	$\Phi_{pred} = 207 + 0.594D + 20.1t - 3.37G$ $R^2 = 78.1\%$ $R^2_{adj} = 64.9\%$

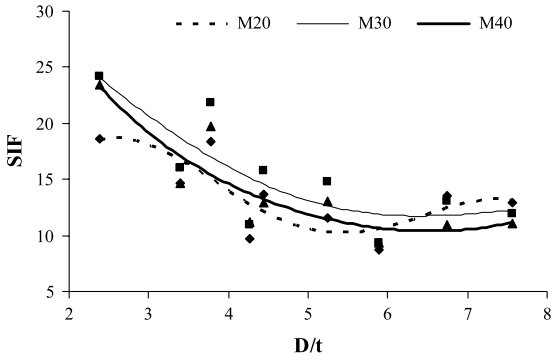

Fig. 4. Variation of strength increasing factor with D/t.

Table 4
Response table for means of mean values of each level of three factors—moment and curvature.

Level	Ultimate moment (kN m)			Curvature at ultimate point (m^{-1})		
	D (mm)	t (mm)	G (N/mm^2)	D (mm)	t (mm)	G (N/mm^2)
1	1.12	1.447	1.723	132.9	121.5	179.9
2	1.95	1.790	1.963	145.2	161.6	135.9
3	2.457	2.290	1.840	143.0	138.0	105.3
Delta	1.337	0.843	0.240	12.3	40.1	74.6
Rank	**1**	**2**	**3**	**3**	**2**	**1**

Table 5
ANOVA table for the response—ultimate moment and curvature at ultimate moment.

Source	DF	Sum of squares		Adj MS		F	
		M_{ue}	Φ_{ue}	M_{ue}	Φ_{ue}	M_{ue}	Φ_{ue}
Diameter	2	2.732	258.0	1.366	129.0	30.31	0.77
Thickness	2	1.079	2441.9	0.539	1221.0	11.97	7.29
Cube strength of concrete	2	0.086	8434.8	0.043	4217.4	0.96	25.17
Error	2	0.090	335.1	0.045	167.6		
Total	8	3.987	11469.9				

Table 7
Accuracy of regression models developed to predict ultimate moments and corresponding curvature—comparison with experimental values.

Sample designation	Moment			Curvature		
	M_{pred} (kN m)	M_{ue} (kN m)	M_{ue}/M_{pred}	Φ_{pred} (m^{-1})	Φ_{ue} (m^{-1})	Φ_{ue}/Φ_{pred}
$D_1t_2M_{20}$	1.03	1.08	1.05	171.88	195.70	**1.14**
$D_1t_3M_{20}$	1.48	1.23	**0.83**	179.92	220.56	**1.23**
$D_1t_1M_{30}$	0.70	0.89	**1.27**	123.73	109.94	**0.89**
$D_1t_3M_{30}$	1.55	1.39	0.90	138.80	167.39	**1.21**
$D_1t_1M_{40}$	0.76	0.86	**1.14**	90.03	77.50	**0.86**
$D_1t_2M_{40}$	1.16	1.19	1.03	97.06	82.43	**0.85**
$D_2t_1M_{20}$	1.52	1.42	0.94	172.39	137.78	**0.80**
$D_2t_2M_{20}$	1.91	1.76	0.92	179.42	159.93	**0.89**
$D_2t_2M_{30}$	1.98	1.98	1.00	138.31	138.75	1.00
$D_2t_3M_{30}$	2.43	2.52	1.04	146.35	145.08	0.99
$D_2t_1M_{40}$	1.64	1.54	0.94	97.57	111.9	**1.14**
$D_2t_3M_{40}$	2.49	2.55	1.02	112.65	143.97	**1.28**
$D_3t_1M_{20}$	1.96	1.80	0.92	176.16	201.32	**1.14**
$D_3t_3M_{20}$	2.80	2.82	1.01	191.23	210.92	1.10
$D_3t_1M_{30}$	2.03	2.03	1.00	135.04	134.29	0.99
$D_3t_2M_{30}$	2.42	2.55	1.05	142.08	136.81	0.96
$D_3t_2M_{40}$	2.48	2.71	1.09	108.38	82.23	**0.76**
$D_3t_3M_{40}$	2.93	3.32	**1.13**	116.42	85.93	**0.74**
Mean			1.02			0.99
Standard deviation			0.10			0.16

Note: (i) M_{ue} and Φ_{ue} values are average of three samples.
(ii) Numbers in bold represent large variations between experimental results and predicted values.

Table 8
Effect of concrete filling on moment capacity of the steel tubes.

D (mm)	t (mm)	Ultimate moment M_{ue} (kN m)				$M_{ue(CFT)}/M_{ue(Hollow)}$		
		Hollow	M_{20}	M_{30}	M_{40}	M_{20}	M_{30}	M_{40}
44.45	1.25	0.48	0.74	0.89	0.86	1.53	**1.85**	1.79
44.45	1.6	0.78	1.08	1.16	1.19	1.38	1.49	1.53
44.45	2	0.89	1.23	1.39	1.46	1.38	1.56	1.63
57.15	1.25	0.74	1.42	1.57	1.54	1.92	**2.13**	2.10
57.15	1.6	1.16	1.76	1.98	2.03	1.51	1.71	1.74
57.15	2	1.76	2.25	2.52	2.55	1.28	1.44	1.45
63.5	1.25	0.85	1.80	2.03	2.03	2.12	**2.38**	2.38
63.5	1.6	1.64	2.18	2.55	2.71	1.32	1.55	1.58
63.5	2	2.25	2.82	3.16	3.31	1.25	1.40	1.45

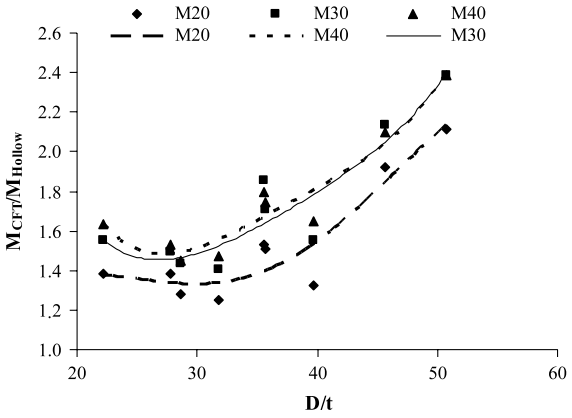

Fig. 5. Flexural performance of CFTs with D/t ratio.

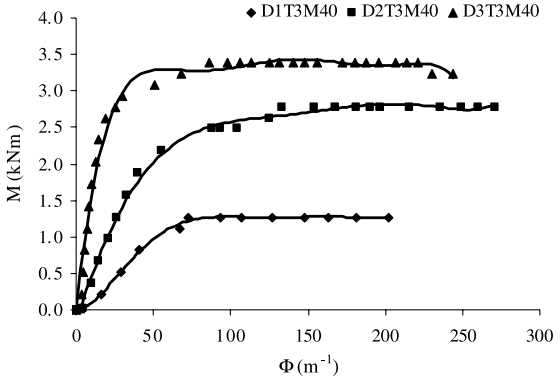

Fig. 6. Moment–curvature relationship—change in cross sectional area of the steel tube.

maximum advantage (M_{CFT}/M_{Hollow}) of filling is obtained for tubes with lowest wall thickness filled with moderate strength concrete. This substantial increase in moment resistance is mainly due to the fact that thinner sections are more susceptible to local buckling as compared to thicker sections. Filling such thin sections with concrete helps in delaying local buckling and hence improves the moment carrying capacity (Fig. 5).

An increase in diameter of the steel tube with a given wall thickness and grade of concrete, helps to increase the ultimate moment capacity due to the increased area of steel and the presence of additional concrete helps in delaying local buckling (Fig. 6).

3.3. Confinement of concrete

Concrete inside the steel tube is confined and the strength of such confined concrete depends upon its own characteristic strength and the thickness of the steel tube. The confinement factor ξ, and **Flexural Strength Index** γ (FSI) proposed by Han-Lin [3] are used to explain the effect of confinement.

Table 9
Effect of concrete filling on curvature of the steel tubes.

D (mm)	t (mm)	Curvature Φ_{ue} (m^{-1})				Relative ductility index [$\Phi_{ue(CFT)}/\Phi_{ue(Hollow)}$]		
		Hollow	M_{20}	M_{30}	M_{40}	M_{20}	M_{30}	M_{40}
44.45	1.25	53.74	157.44	109.94	77.50	**2.93**	2.05	1.44
44.45	1.6	72.56	161.27	141.07	82.43	2.22	1.94	1.14
44.45	2	77.50	220.56	175.58	100.14	2.85	2.27	1.29
57.15	1.25	75.52	138.17	126.53	111.90	**1.83**	1.68	1.48
57.15	1.6	98.18	160.32	139.14	135.26	1.63	1.42	1.38
57.15	2	99.16	173.68	144.93	143.97	1.75	1.46	1.45
63.50	1.25	53.74	201.04	134.29	80.46	**3.74**	2.50	1.50
63.50	1.6	58.70	208.51	137.20	82.43	3.55	2.34	1.40
63.50	2	64.64	211.30	140.10	86.38	3.27	2.17	1.34

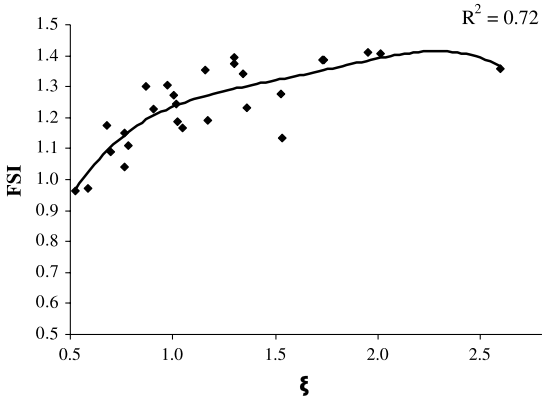

Fig. 7. Variation of flexural strength index with confinement factor.

$$\xi = \frac{A_s.f_y}{A_c.f_{ck}} \tag{2}$$

where A_s and A_c are the cross-sectional area of the steel and concrete core, f_y and f_{ck} are the yield stress of steel and characteristic compressive strength of concrete

$$\gamma = \frac{M_u}{W_{scm}.f_{scy}} \tag{3}$$

where W_{scm} = Section modulus of the composite beams; given by $\pi D^3/32$; M_u = Moment capacity of the composite beams; f_{scy} = Nominal yielding strength, defined as; $f_{scy} = (1.14 + 1.02\xi)f_{ck}$.

FSI is a measure of moment capacity of a given section with given geometrical and material strength properties. From Fig. 7 it is observed that the FSI increases with increase in confinement factor up to certain extent and this indicates that better confinement leads to a higher FSI. Hence CFT samples with higher grades of in-fill concrete have performed better only when the wall thickness of the steel tube is also correspondingly increased. In other words the confinement factor is increased. A decrease in the FSI beyond a certain limit (1.4) indicates that an increase in the wall thickness of the steel tube combined with a lower strength of in-fill concrete has no beneficial effect on moment capacity of the CFT sections.

3.4. Curvature

Curvature is used to describe the ductility of the hollow and composite samples. From Table 9, it is observed that the ductility of the hollow samples is increased due to concrete filling. It is found that with an increase in strength of in-filled concrete, the ductility of CFT beams is decreased; however an increase in wall thickness could decrease this effect to a certain extent. The ductility of CFTs as compared to hollow steel tubes (Table 9) is expressed as **Relative Ductility Index** (RDI) and is defined as the ratio of curvature at ultimate moment of CFT to that of the corresponding hollow steel tube.

Table 10
Comparison of experimental moment capacity values with predicted values from EC4, AISC-LRFD.

D (mm)	t (mm)	M_{ue}/M_{EC4}			M_{ue}/M_{AISC}		
		M_{20}	M_{30}	M_{40}	M_{20}	M_{30}	M_{40}
44.45	1.25	1.10	1.29	1.22	1.26	1.53	1.48
44.45	1.6	1.30	1.36	1.37	1.47	1.58	1.62
44.45	2	1.24	1.36	1.40	1.37	1.54	1.62
57.15	1.25	1.23	1.32	1.27	1.45	1.61	1.58
57.15	1.6	1.24	1.35	1.35	1.42	1.61	1.64
57.15	2	1.31	1.43	1.42	1.48	1.66	1.68
63.5	1.25	1.25	1.36	1.33	1.49	1.67	1.67
63.5	1.6	1.22	1.38	1.38	1.42	1.66	1.69
63.5	2	1.31	1.42	1.44	1.49	1.67	1.72
Mean		1.32			1.56		
Standard deviation		0.08			0.11		

$$\text{Relative Ductility Index (RDI)} = \frac{\phi_{\text{CFT}}}{\phi_{\text{Hollow}}}. \tag{4}$$

Thin steel tubes with a lower strength concrete (M_{20}) have shown higher RDI values. During the experiments, with an increase in transverse load there is an increase in deflection of the CFT. CFTs having a thin steel tube with lower strength concrete, sustain a large deflection. But once the in-fill concrete fails, the thin steel tube buckles and it will not bear the additional transverse load. This is evident from the experimental results by observing an increased deflection of the CFTs under a constant or small drop in ultimate lateral load. But in case of thin steel tubes filled with higher strength concrete, the CFT failed at a smaller deflection at ultimate load due to the brittle nature of the concrete and shows lower ductility.

3.5. Comparison of test results with EC4 and AISC-LRFD

The moment capacities of the specimens are calculated based on the specifications in the EC4-1994. The safety factors in the specifications were set to unity so that the predicted values obtained in the codes could be used for comparison with the experimental ultimate bending moments. From Table 10, it is observed that EC4-1994 conservatively predicts the moment capacity of CFT sections used in the present experimental investigation with a mean value of 1.32 and is consistent with standard deviation of 0.08 for M_{ue}/M_{EC4}. AISC-LRFD provisions do not consider the effect of concrete in-fill and hence the predicted moment capacity values of the CFT samples are again much lower as compared to the present experimental values (Table 10).

3.6. Comparison of test results with models by Han-Lin and Elchalakani et al.

Moment capacity of all the test samples are again determined by the theoretical models proposed by Han-Lin [3] and Elchalakani et al. [1]. While the experimental validity limits of the equation

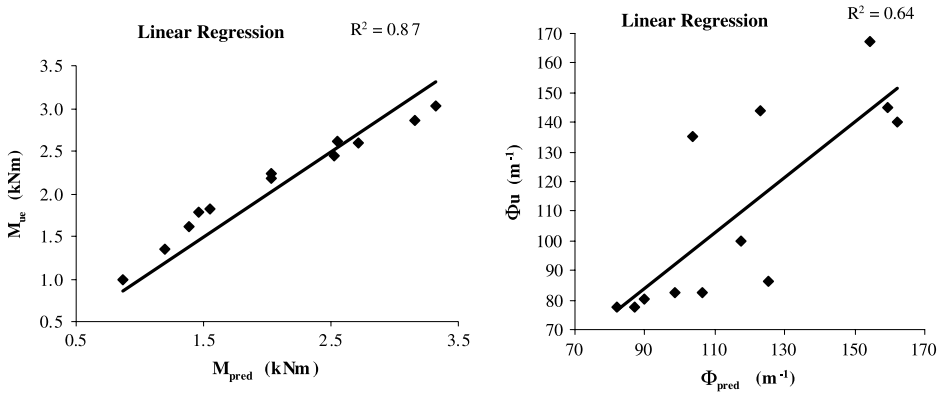

Fig. 8. Predicted moment capacity and curvature values vs. experimental results—linear regression analysis.

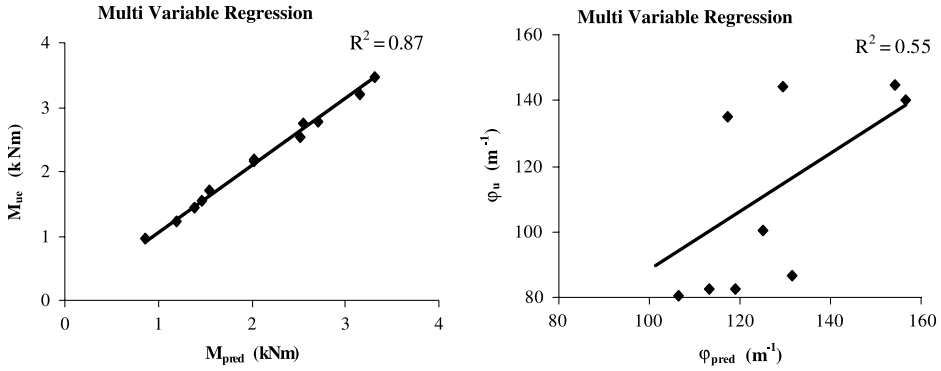

Fig. 9. Predicted moment capacity and curvature values vs. experimental results—Multi-variable regression analysis.

Table 11
Comparison of experimental moment capacity values with predicted values from Han model and Elchalakani model.

D (mm)	t (mm)	M_{ue}/M_{Han}			$M_{ue}/M_{Elchalakani}$		
		M_{20}	M_{30}	M_{40}	M_{20}	M_{30}	M_{40}
44.45	1.25	0.81	0.97	0.92	1.16	1.45	1.46
44.45	1.6	0.90	0.97	0.99	1.34	1.46	1.53
44.45	2	0.79	0.90	0.95	1.26	1.41	1.50
57.15	1.25	0.95	1.03	0.98	1.35	1.60	1.68
57.15	1.6	0.91	1.02	1.02	1.31	1.52	1.62
57.15	2	0.92	1.02	1.02	1.36	1.53	1.59
63.5	1.25	0.98	1.07	1.03	1.40	1.71	1.85
63.5	1.6	0.92	1.06	1.05	1.31	1.60	1.79
63.5	2	0.94	1.05	1.06	1.36	1.56	1.69
Mean		0.97			1.5		
Standard deviation		0.07			0.17		

proposed by Han-Lin [3] are $D = 100$–200 mm, it is seen that the model estimates quite satisfactorily the moment capacity of the CFT samples tested herein, even though they have diameters in the range of 44.45–63.5 mm. The estimates are within ± 10% of the experimental values (Table 11).

Again a simplified formula proposed by Elchalakani et al. [1] is used to predict the moment capacity of the CFTs tested herein. The proposed formula may not be taking the effect of strength of in-fill concrete for steel tubes having lower yield strength value of 250 MPa and with D/t limits of 22.3 to 50.8. It is found that the predicted estimates are much too conservative as compared to actual ultimate moments (Table 11).

3.7. Regression analysis method for predicting ultimate moment capacity and curvature of the CFT beams

With the help of the Statistical Package for Social Science (SPSS-version 10), a regression analysis is performed and linear regression models are proposed to calculate the ultimate moment and the corresponding curvature [Eqs. (5) and (6)]. About 56% of the data is used to develop the model and the remaining data is used to compare the predicted values with experimental results (Fig. 8). It is seen from statistical models that moment capacity is predicted satisfactorily, while the model developed for curvature shows a slightly lower correlation.

3.7.1. Linear regression model to predict moment and curvature

$$\text{Ultimate moment} = -4.065 + 0.065D + 1.06t + 0.016G \quad (5)$$

$R^2 = 0.977 \qquad R^2_{adj} = 0.971.$

$$\text{Curvature at ultimate point} = 187.76 + 0.413D + 47.411t - 3.667G \quad (6)$$

$R^2 = 0.730 \qquad R^2_{adj} = 0.656.$

It is interesting to note that the coefficients of the important parameters in the above regression equations for moment and curvature are comparable to coefficients in the earlier regression equation (Table 6) based on Taguchi's DOE approach. This suggests that Taguchi's DOE approach can be effectively used in these types of experiment.

3.7.2. Multi variable regression models to predict moment and curvature

On similar lines, Multivariable Regression Models (MVR) are also developed to predict moment capacity and curvature of circular CFTs [Eqs. (7) and (8)]. Plots of predicted values against experimental results are shown in Fig. 9, where again it can be seen that predictions are satisfactory for ultimate moment but not so for the corresponding curvature.

$$\text{Ultimate moment} = (10)^{-4.44}(D)^{2.26}(t)^{1.006}(G)^{0.36} \quad (7)$$

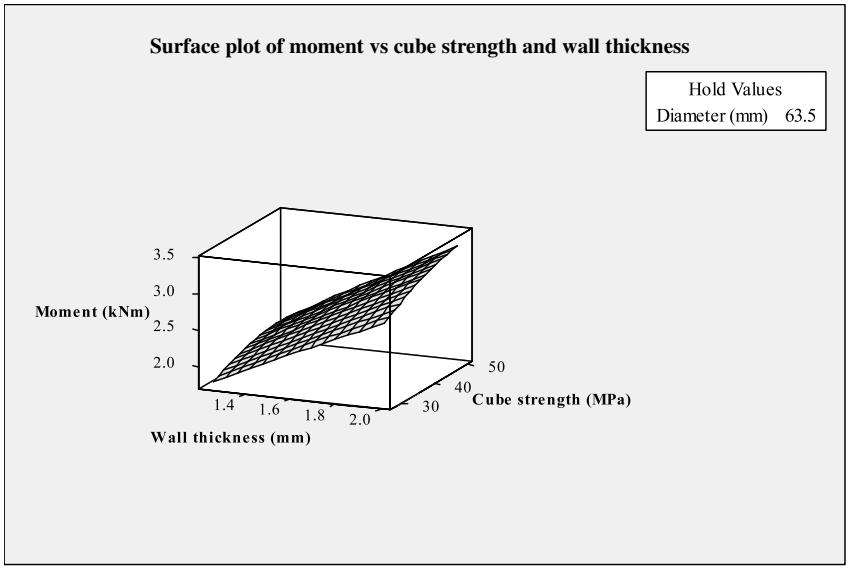

Fig. 10. Surface response plot of moment vs. cube strength and wall thickness for a CFT of 63.5 mm diameter.

$R^2 = 0.994 \quad R^2_{adj} = 0.993.$

$$\text{Curvature at ultimate point} = (10)^{3.06}(D)^{0.14}(t)^{0.45}(G)^{-0.78} \quad (8)$$

$R^2 = 0.757 \quad R^2_{adj} = 0.691$

where G = Cube strength of the in-fill concrete.

3.8. Interaction model for moment capacity and curvature of the CFT beams

Moment capacity and corresponding curvature of the circular CFTs are mainly influenced by three variables diameter, wall thickness and grade of concrete. It can be argued that there must be an interaction of these parameters in deciding the moment capacity and curvature. Hence, based on experimental results, the interaction of these parameters on structural responses is determined from the Response Surface Method using MINITAB (version 14). Such interaction formulae developed are given in Eqs. (9) and (10).

$$\begin{aligned}\text{Ultimate moment} &= 3.276 - 0.135D - 1.367t + 0.008G \\ &+ 0.001D^2 - 0.088t^2 - 0.0006G^2 + 0.043Dt \\ &+ 0.0006DG + 0.011tG \end{aligned} \quad (9)$$

$R^2 = 0.997 \quad R^2_{adj} = 0.995.$

$$\begin{aligned}\text{Curvature at ultimate point} &= -24.726 - 0.267D + 312.527t \\ &- 2.155G + 0.045D^2 - 36.445t^2 - 0.013G^2 - 2.540Dt \\ &- 0.007DG - 0.306tG \end{aligned} \quad (10)$$

$R^2 = 0.840 \quad R^2_{adj} = 0.760.$

The proposed equations are used to calculate the moment capacity of the CFT samples used in the experimental investigations carried out by W.M. Gho and Dalin Liu [2] and Han-Lin [3]. The Multivariable Regression Model and interaction models proposed for circular CFTs are used to predict the moment capacity of rectangular CFTs by considering the equivalent diameter for rectangular cross-sectional area. It is found that the Multivariable Regression Model predicts the moment capacity of rectangular CFTs with mean value of $M_{ue}/M_{model} = 1.11$, while the interaction model agrees with the test results of Han-Lin [3] with a mean value of $M_{ue}/M_{model} = 1.33$ (Table 12). Predicted results with interaction model and test results of Gho W.-M. and Dalin Liu [2] do not show a good correlation.

Typical Response Surface plots and Contours plots for moment capacity and curvature have been drawn using MINITAB (version 14). Plots indicate the effect of variables on an individual response (Figs. 10–13). Contour plots are useful to arrive at a proper combination of tube diameter, wall thickness and strength of in-fill concrete for the given values of moment and curvature of CFTs.

3.9. Failure modes

Different modes of failure as observed for hollow and CFT flexural test specimens during the experimental investigations can be summarised as below.

- Hollow sections have failed with inward local buckling at compression face (Fig. 14).
- There is a substantial change in the post yield behaviour and failure pattern of the test specimens when they are filled with concrete (Fig. 15).
- The CFT specimens failed by local outward buckling of steel skin after breaking of the bond between steel and concrete and ripples are seen on the compression face at ultimate load (Fig. 15).

4. Conclusions

Results of experimental investigations of circular hollow and concrete filled samples with a D/t ratio 22.3–50.8 have been presented in this paper. From the experimental results and detailed analysis carried out, the following broad conclusions can be drawn

(1) A substantial increase in the moment of resistance and the corresponding curvature of all the hollow sections used in the experimental investigation are observed due to concrete filling and the CFT specimens exhibited a higher ductility than the hollow sections. An increase in the wall thickness of the steel tube increases the moment of resistance and ductility of both the hollow and CFT samples.

(2) Regression models developed based on the results of a minimum number of experiments carried out using Taguchi's DOE approach can be adopted for the critical design of CFT beams under flexure.

(3) An increase in strength of in-filled concrete for a given wall thickness of a CFT specimen, does not help in increasing the moment carrying capacity to a great extent. The parameter Strength Increasing Factor, proposed herein helps to estimate

Table 12
Comparison of test results with predicted beam strengths using the proposed regression models.

Cross section (mm)	Cube strength of concrete (N/mm^2)	Experimental moment capacity M_{ue} (kN m)	Formula (7) M_{u7} (kN m)	M_{ue}/M_{u7}	Formula (9) M_{u9} (kN m)	M_{ue}/M_{u9}	Test data source
120 × 120 × 3.84	23.6	30.16	28.39	1.06	23.23	1.29	Han Lin [3]
120 × 120 × 5.86	26.8	41.43	45.45	0.91	31.49	1.31	
150 × 120 × 2.93	23.1	31.4	27.62	1.14	24.39	1.28	
120 × 90 × 2.93	23.1	21.1	15.50	1.36	14.41	1.46	
Mean				1.11		1.33	
149.9 × 150.3 × 4.88	56.3	81.8	81.50	1.00	45.14	1.81	W.M. Gho and Dalin Liu [2]
150.2 × 150.2 × 4.92	87.5	98.4	96.52	1.02	47.92	2.05	
250.1 × 148.8 × 5.85	90.9	217.7	204.86	1.06	81.86	2.66	
Mean				1.02		2.17	

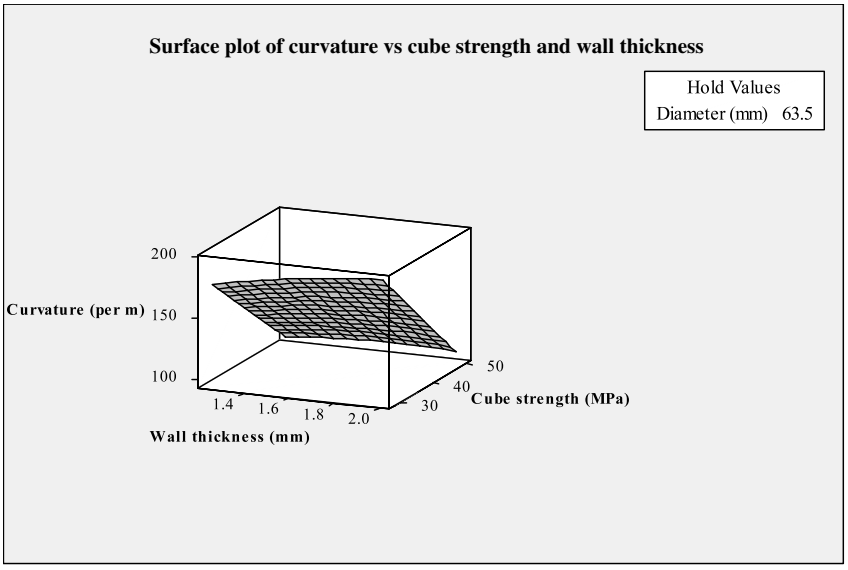

Fig. 11. Surface response plot of curvature vs. cube strength and wall thickness for a CFT of 63.5 mm diameter.

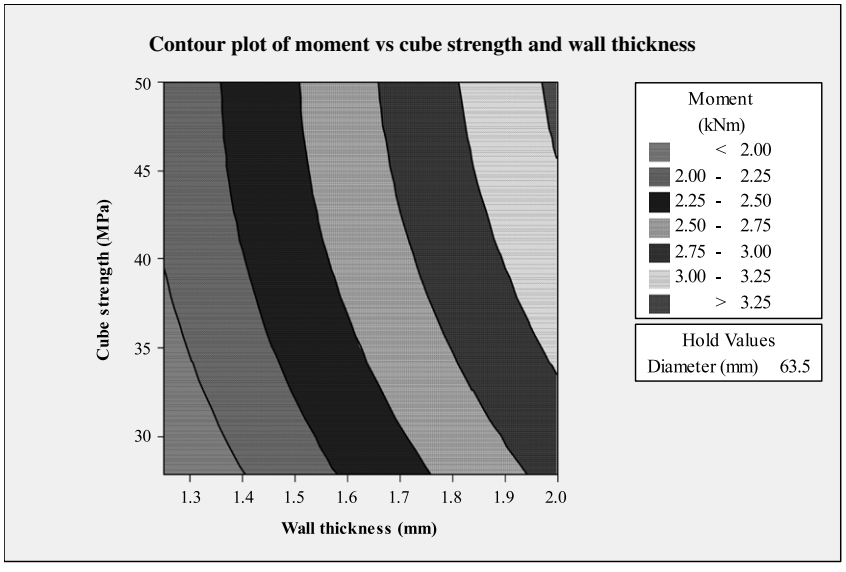

Fig. 12. Contour plot of moment vs. cube strength and wall thickness for a CFT of 63.5 mm diameter.

the contribution of concrete for the moment capacity of CFT beams. The confinement of in-fill concrete contributes to a higher performance when a higher strength of in-fill concrete is used with a steel tube of higher wall thickness.

(4) EC4-1994 predicts the moment capacity of test samples conservatively up to an extent of 30%–35%. AISC-LRFD is also highly conservative in predicting the moment capacity of the CFT sections since effect of concrete in-fill is not considered in the same.

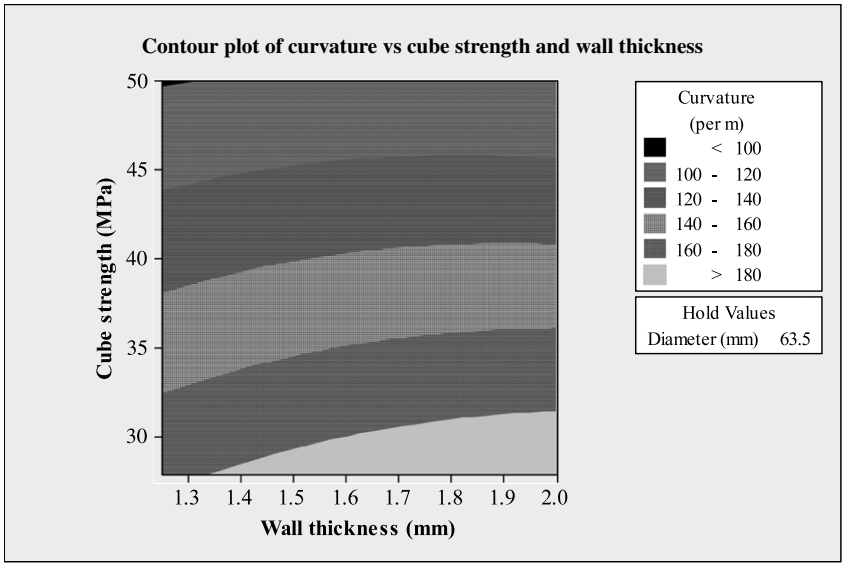

Fig. 13. Contour plot of curvature vs. cube strength and wall thickness for a CFT of 63.5 mm diameter.

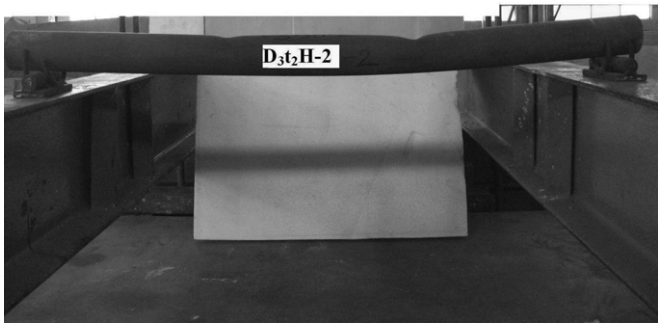

Fig. 14. Failure of hollow sample with inward local buckling at compression face.

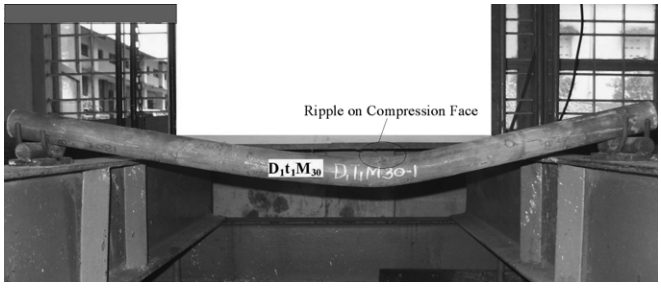

Fig. 15. CFT sample at failure — Overall buckling mode.

(6) The Multi-Variable Regression Model predicts the ultimate moment capacity of CFTs fairly well. The interaction model proposed in the present study estimates the effect of different variables on ultimate moment capacity and corresponding curvature of circular CFT beams.

Acknowledgement

The authors are grateful to M/s Shankara Pipes Private Limited, Bangalore, INDIA for providing all the steel tubes used in the experimental programme.

References

[1] Elchalakani M, Zhao XL, Grzebieta RH. Concrete-filled circular steel tubes subjected to pure bending. Journal of Constructional Steel Research 2001;57:1141–68.
[2] Gho Wie-Min, Liu Dalin. Flexural behavior of high-strength rectangular concrete-filled steel hollow sections. Journal of Constructional Steel Research 2004;60:1681–96.
[3] Han Lin-Hai. Flexural behaviour of concrete-filled steel tubes. Journal of Constructional Steel Research 2004;60:313–37.
[4] Bridge RQ. Concrete filled steel tubular columns. Report no. R283. Sydney (Australia): School of Civil Engineering, University of Sydney; 1976.
[5] Lu YQ, Kennedy DJL. The flexural behavior of concrete-filled hollow structural sections. Canadian Journal of Civil Engineering 1994;21(1):11–130.
[6] Uy B. Strength of concrete filled steel box columns incorporating local buckling. Journal of Structural Engineering, ASCE 2000;126(3):341–52.
[7] Elremaily A, Azizinamini A. Behavior and strength of circular concrete-filled tube columns. Journal of Constructional Steel Research 2002;58:1567–91.
[8] American Institute of Steel Construction (AISC), Manual of steel construction: Load and resistance factor design (LRFD). 2nd ed. Chicago. 1994.
[9] IS 10262-1982. Indian standard recommended guidelines for concrete mix design. Bureau of Indian Standards, New Delhi, India.
[10] Eurocode 4. Design of composite steel and concrete structures, part 1.1: General rules and rules for buildings (together with United Kingdom National Application Document). DD ENV 1994-1-1:1994. London W1A2BS: British Standards Institution; 1994.
[11] Douglas Montgomery. Design and analysis of experiments. 5th ed. New York: John Wiley & Sons (ASIA) Pvt. Ltd.; 2004.
[12] IS 456-2000 plain reinforced concrete-code of practice. New Delhi, India; Bureau of Indian Standards.